Journal of the Physical Society of Japan **83**, 034007 (2014)
http://dx.doi.org/10.7566/JPSJ.83.034007

Effect of Negatively Charged Impurity on Graphene Magnetic Rings

Chak Man Lee[1,2*], Kwok Sum Chan[1,2†], and Johnny Chung Yin Ho[1,2]

[1]*Department of Physics and Materials Science and Center for Functional Photonics, City University of Hong Kong, Tat Chee Avenue, Kowloon, Hong Kong, People's Republic of China*
[2]*City University of Hong Kong Shenzhen Research Institute, Shenzhen, People's Republic of China*

(Received September 11, 2013; accepted January 6, 2014; published online February 24, 2014)

Using the massless Dirac–Weyl model of monolayer graphene, we study the effect of a negatively charged Coulomb impurity on the low-lying spectra of single-electron magnetic dot and ring systems. The numerical results show that the electron–hole symmetry in the spectra is broken by the Coulomb potential, and the original degenerate energy level lying at zero energy becomes nondegenerate and splits into infinite discrete angular momentum states, which have positive energies and thus are electron-like. For higher LLs, each has a reverse ordering of the energy levels when r_{02}^2/a^2 is larger than its critical value in the positive energy states for magnetic dot systems owing to the competition between the Coulomb potential and the magnetic confinement.

1. Introduction

In recent years, graphene has generated much research interest, both experimental and theoretical, according to a review,[1)] since its isolation in laboratories.[2,3)] Owing to its exceptionally high carrier mobility and structural stability even without protection from the surroundings under ambient conditions, it is regarded as a promising candidate material for nanoscale electronic devices, as well as for high-density memory devices and spintronic devices.

For electronic devices, the first consideration is the confinement of electrons using either electric or magnetic methods or both. For graphene, the incomplete electric confinement of its massless carriers due to Klein tunneling[4)] is a limitation in electronic device application, since carriers can propagate via quasi-hole states and be transmitted perfectly through a barrier. Magnetic confinement is a possible alternative approach to overcoming this difficulty, since the magnetic field deflects the trajectories of charged carriers through the Lorentz force, trapping the carriers within a small region.

In uniform fields, the low-lying spectra obtained using the relativistic Dirac–Weyl (DW) model, as appropriate for graphene, are different from those obtained using the nonrelativistic Schrödinger model. For the former model, low-lying Landau levels (LLs) with eigenenergies $E \propto \sqrt{BN}$ where N is the LL index, are proportional to the square root of the magnetic field B with unequal level spacings under a fixed magnetic field, while, for the latter model, LLs with $E \propto B(N + 1/2)$ are linear with equal spacings.

For the DW model, Martino and coworkers previously gave an interesting proposal to confine electrons by inhomogeneous magnetic fields.[5–7)] Various inhomogeneous magnetic field configurations were subsequently suggested to confine electrons, such as exponentially decaying fields,[8)] non-zero fields in a circular dot,[9)] fields corresponding to various potentials,[10)] circular step fields,[11)] Gaussian fields,[12)] ring fields,[13)] and even the presence of Coulomb impurities under uniform fields.[14,15)] In all these studies, discontinuous and/or inhomogeneous magnetic fields were considered focusing on the field dependence of the low-lying spectra and the energy dependence of the transmission probability through the magnetic barriers, as well as the electron states, which include bound, quasi-bound and scattering states. They conclude that electrons can be confined by magnetic barriers in graphene. The doping of extrinsic impurities into these systems is another important topic in the study of graphene since it can modify the energy levels, which may largely affect its electronic structure and optical properties. However, studies of the above-mentioned configurations with impurities in more realistic situations are few.

In the present study, we modify the original DW equations for monolayer graphene by adding a Coulomb interaction term for a negative point charge at the center of the magnetic dot or ring system into the two diagonal matrix elements of the DW Hamiltonian, just like a negatively charged Coulomb impurity in a realistic experimental situation. Owing to the presence of these terms, the Hamiltonian can only be simplified but not decoupled into two equations. Different from that in a previous work,[13)] we first rearrange the two nondiagonal matrix elements separately and consider that part with the raising operator $\hat{\pi}_0^+$ and the lowering operator $\hat{\pi}_0^-$ as the unperturbed Hamiltonian [see Eq. (4)]. The corresponding eigenvectors for these two operators are exactly the same as the two-dimensional (2D) harmonic product basis states, which are used to form the model space. The low-lying spectra of the single-electron magnetic ring and dot systems are then calculated using the bases. Finally, we compare and analyse our overall numerical results for these two systems with and without an impurity. Note that previous experimental studies[16–18)] of the effect of magnetic field modulation on a nonrelativistic two-dimensional electron gas (2DEG) may be used to experimentally achieve our theoretical findings.

2. Theory

The massless DW Hamiltonian describing a single electron bound to an on-center negatively charged Coulomb impurity in a 2D monolayer graphene based magnetic dot or ring formed by a magnetic field is[14,15)]

$$\hat{H} = v_F \sigma \cdot (\mathbf{P} + e\mathbf{A}) + \frac{e^2}{4\pi\epsilon r}\mathbf{I}, \tag{1}$$

where v_F is the electron's Fermi velocity instead of the photon's in the conventional Dirac equation. $\sigma = (\sigma_x, \sigma_y)$ and $\mathbf{I}$ are the 2×2 Pauli matrices in the pseudospin space, and the identity matrix, respectively. $\mathbf{P}$ and $\mathbf{A}$ are the momentum operator and the vector potential in the 2D space,

respectively. Both the diagonal matrix elements for the last term of the DW Hamiltonian denote the Coulomb interaction between the electron and the on-center impurity. The positive sign of the Coulomb interaction is for repulsion. Note that, for mathematical simplicity, both the electron–electron interaction and the Zeeman term for the coupling of the electron spin and the magnetic field are neglected.

In realistic experimental situations, the magnetic ring is formed by an inhomogeneous magnetic field: the magnetic field perpendicular to the xy plane within the ring region is zero, i.e., $B(r) = 0$ for $r_{01} \le r \le r_{02}$, and a constant B outside it, i.e., $B(r) = B_0\hat{e}_z$, where $\hat{e}_z$ is the unit vector in the z-direction, and r_{01} and r_{02} are the inner and outer radii of the magnetic ring, respectively. Such a magnetic field profile can be realized by placing the same shape of thin superconducting material below the transition temperature on top of the graphene so that the magnetic field is expelled from the superconducting material, leading to an inhomogeneous field profile on the graphene. For circular symmetry, by using the relationship of the magnetic flux $\Phi(r)$ $[= 2\pi rA(r)]$ and the area integral of $B(r)$, the corresponding vector potential $\mathbf{A}$ in the polar coordinate representation is then given by[19,20]

$$\mathbf{A} = \begin{cases} \dfrac{B_0}{2}\hat{e}_z \times \mathbf{r} & \text{for } 0 \le r < r_{01}, \\ \dfrac{B_0 r_{01}^2}{2r^2}\hat{e}_z \times \mathbf{r} & \text{for } r_{01} \le r \le r_{02}, \\ \dfrac{B_0(r^2 - (r_{02}^2 - r_{01}^2))}{2r^2}\hat{e}_z \times \mathbf{r} & \text{for } r > r_{02}. \end{cases} \quad (2)$$

When the inner radius r_{01} approaches zero, the resulting vector potential can be reduced to the case of a magnetic dot with the radius r_{02}.

In order to calculate the eigenenergy of the whole single electron system by numerical diagonalization, the Hamiltonian Eq. (1) is decomposed into two parts:

$$\hat{H} = \hat{H}_0 + \hat{V}. \quad (3)$$

The unperturbed Hamiltonian $\hat{H}_0$ as a 2×2 matrix is extracted from $\hat{H}$ such that $\hat{H}_0$ describes an electron moving in the absence of the Coulomb impurity under a uniform field B_0, which can be expressed as

$$\hat{H}_0 = v_{\mathrm{F}} \begin{pmatrix} 0 & \hat{\pi}_0^- \\ \hat{\pi}_0^+ & 0 \end{pmatrix}, \quad (4)$$

with

$$\hat{\pi}_0^{\pm} = \pm j \exp(\pm j\theta)\left[\mp\hbar\frac{\partial}{\partial r} + \frac{l\hbar}{r} + \frac{erB_0}{2}\right]. \quad (5)$$

$\hat{H}_0$ can be solved analytically, having the well-known 2D harmonic product basis states, which are the two components of the spinor eigenfunctions. With the radial quantum number n, the orbital angular momentum $l\hbar$, and the imaginary unit j, the two-component spinor can be expressed as

$$\Psi_{nl}^T = (\phi_{N-1,l-1} \;\; j\phi_{N,l}), \quad (6)$$

where the nonnegative integer LL index is N $[\equiv n + (l + |l|)/2]$ and

$$\phi_{N,l} = 1/\sqrt{2\pi}e^{jl\theta}\left[\frac{n!}{a^2(n+|l|)!}\right]^{1/2} \times (r/\sqrt{2}a)^{|l|}L_n^{|l|}(r^2/2a^2)e^{-r^2/4a^2}. \quad (7)$$

The corresponding two eigenvalues are respectively $E_{N,l} = +N^{\frac{1}{2}}$ and $-N^{\frac{1}{2}}$ in energy unit of $\hbar\omega$ $(\equiv \sqrt{2}v_{\mathrm{F}}\hbar/a)$. In Eq. (7), θ is the azimuthal angle on the xy plane. $L_n^{|l|}$ and a $(\equiv \sqrt{\hbar/eB_0})$ are the associated Laguerre polynomials and magnetic length, respectively. Note that, as can be seen from the eigenvalues for uniform fields, $\hat{\pi}_0^-$ and $\hat{\pi}_0^+$ can be regarded as the lowering and raising operators, respectively, i.e., $\hat{\pi}_0^+\phi_{N-1,l-1} = \sqrt{N}\phi_{N,l}$ and $\hat{\pi}_0^-\phi_{N,l} = \sqrt{N}\phi_{N-1,l-1}$. From Eq. (6), the first spinor component is set to zero for the LL index $N = 0$, since it is a nonnegative integer. For the LL, note that each bulk LL under a uniform magnetic field is degenerate and consists of infinite quantum states with various orbital angular momenta (l) depending on their LL index N. In order to differentiate them from the bulk LLs, under nonuniform magnetic fields, these discrete quantum states split from the bulk LL are called the angular momentum states.

The 2×2 matrix block of the remaining part of the Hamiltonian $\hat{V}$ from Eq. (3), the residual potential, can then be expressed as

$$\hat{V} = \begin{pmatrix} \hat{V}_{\mathrm{coul}} & \hat{V}_+ \\ \hat{V}_- & \hat{V}_{\mathrm{coul}} \end{pmatrix}, \quad (8)$$

in which the four matrix elements are given by

$$\hat{V}_{\mathrm{coul}} = C\frac{1}{r}, \quad (9)$$

$$\hat{V}_{\pm} = \mp j\exp(\mp j\theta) \times \begin{cases} 0 & \text{for } 0 \le r < r_{01}, \\ -\dfrac{1}{2\sqrt{2}r}(r^2 - r_{01}^2) & \text{for } r_{01} \le r \le r_{02}, \\ -\dfrac{1}{2\sqrt{2}r}(r_{02}^2 - r_{01}^2) & \text{for } r > r_{02}, \end{cases} \quad (10)$$

where, in the diagonal term [Eq. (9)], the Coulomb parameter C represents the interaction strength of the electron with the on-center impurity and is given by

$$C = \frac{e^2}{2\sqrt{2}\epsilon v_{\mathrm{F}}h} \quad (11)$$

in unit of the magnetic length. The phase factors $\exp(\pm j\theta)$ are cancelled off during the integration of the corresponding matrix elements, since the orbital angular momenta of the two spinor components involved differed by one [see Eq. (6)].

The above formalism, as a whole, is different from that of the impurity-free case.[13] Several notes worth mentioning are that, (a) since the Hamiltonian, a 2×2 matrix due to the presence of an impurity cannot decouple into two separate equations, the basis vectors have to be used in pairs in the model space [see Eq. (6)] in the direct diagonalization. (b) The perturbation terms due to the inhomogeneous magnetic field $\hat{V}_{\pm}$ are very different from those in the impurity-free case [see Eq. (7) in Ref. 13], since in the latter case, taking the square of the Hamiltonian is required for decoupling the equations before the diagonalization.

In the numerical calculation, the accuracy of the solutions obtained using diagonalization depends on the size of the model space. However, the larger the size of the model space used to obtain reliable results with satisfactory convergence, the lower the computational efficiency is. In our present work, the model space for the 2×2 matrix Hamiltonian

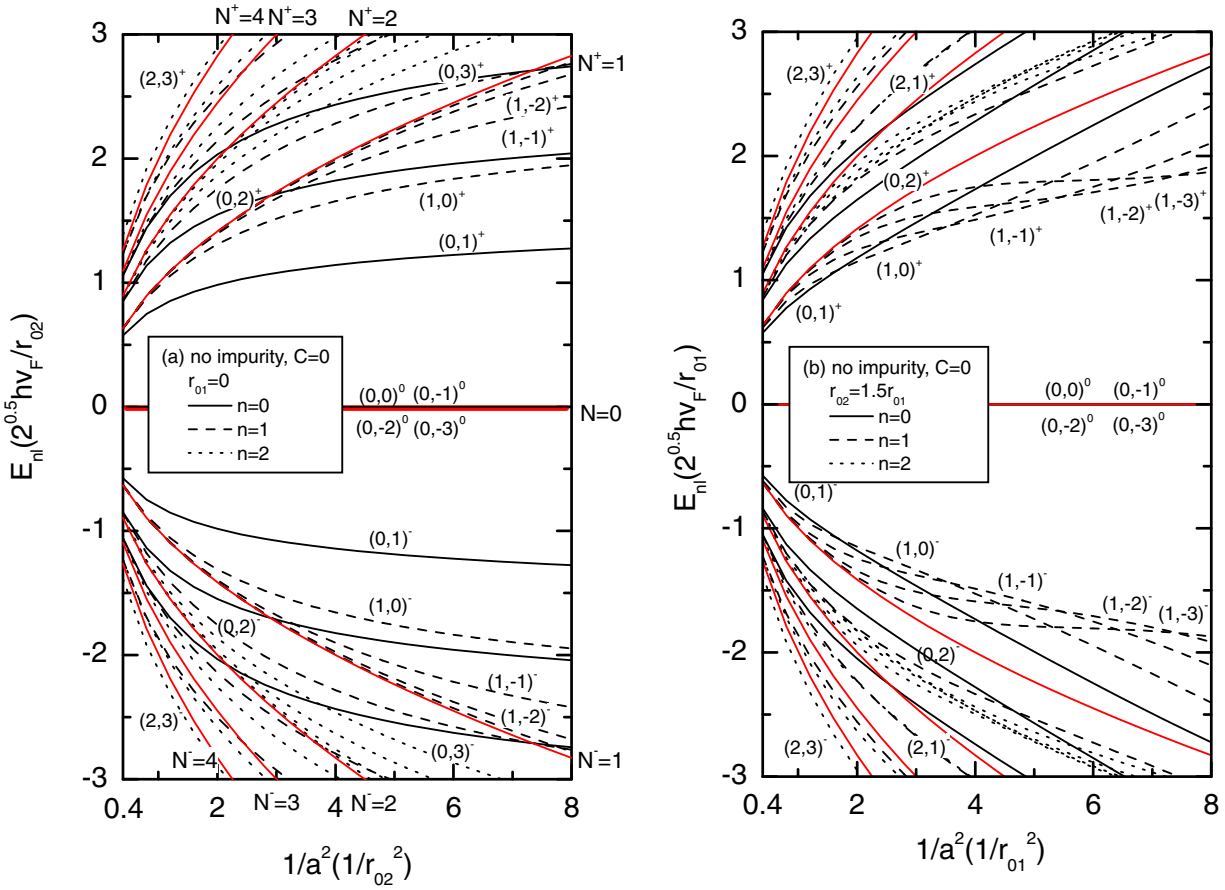

Fig. 1. (Color online) Low-lying spectra of (a) a magnetic dot and (b) a magnetic ring as functions of $1/a^2$, which is proportional to the magnetic field ($\propto B_0$), without impurity, i.e., Coulomb parameter $C = 0$, noting that several low bulk LLs (up to $N = 4$ from zero) denoted by solid curves in red are drawn for comparison.

[Eq. (8)] has 30 pairs of the low-energy eigenstates for a particular orbital angular momentum, l.

3. Discussion and Conclusions

Our numerical results are limited to the quantum states $0 \leq n \leq 2$ and $|l| \leq 3$, which still show major differences in features between the magnetic dot and the magnetic ring, even though higher quantum states are not considered. In actual diagonalization for a particular l, in the case of no impurities, pairs of eigenenergies of the electron and the hole states can be easily identified since they are in pairs with opposite signs. However, in the presence of an impurity, the eigenvalues for the corresponding lowest quantum states (n, l) have to be extracted with much care, since the whole low-lying spectra shift upward owing to the repulsive impurity. The levels in the spectra still appear in pairs, but are different not just by having opposite signs, owing to the breaking of the electron–hole symmetry. In all the figures, the states are labeled $(n, l)^{\pm}$, for which the superscripts "$\pm$" represent the electron (or positive energy) and hole (or negative energy) states, respectively, while the original highly degenerate zero-energy states as exceptions are denoted by the superscript "0". Using the impurity-free case[13] (see Fig. 1) as reference, Figs. 2, 3, and 4 show how the low-lying spectra change in both the (a) magnetic dot and (b) ring systems, when the Coulomb interaction strength between the electron and on-center impurity increases.

We discuss our numerical results primarily on the basis of the following four important observations of the underlying physics. (1) The effect of the magnetic field is to push the electron toward the center of the system, particularly as a result of the factor $\exp(-r^2/4a^2)$ in Eq. (7). (2) The average orbit size for an electron moving around the center is given by the mean square orbit radius $\langle r^2 \rangle \propto 2n + |l| + 1 = 2N - l + 1$. For a certain field, the smaller the value of $-l$ for a given LL, the closer the electron orbit is to its center. (3) Different angular momentum states exist within the dot or ring region under different magnetic fields, causing the angular momentum states to deviate from their corresponding bulk LLs. (4) For a repulsive impurity, there is an increase in the eigenenergy and a shift of the low-lying spectra upward.

Let us now consider the zero-energy states for both the magnetic dot and ring systems. Figures 2 to 4 show the low-lying spectra in the case of a negatively charged impurity. As can be clearly seen, the originally highly degenerate LL ($N = 0$), different from those of the impurity-free cases in Fig. 1,[12,13] becomes nondegenerate and splits into discrete angular momentum states or electron-like states. When the Coulomb interaction increases, these angular momentum states shift upward and move further away from the zero bulk LL, owing to the electron-impurity repulsion. As shown in these figures, the $(0, 0)^0$ state is much higher than its neighbouring states; this is because this state has no

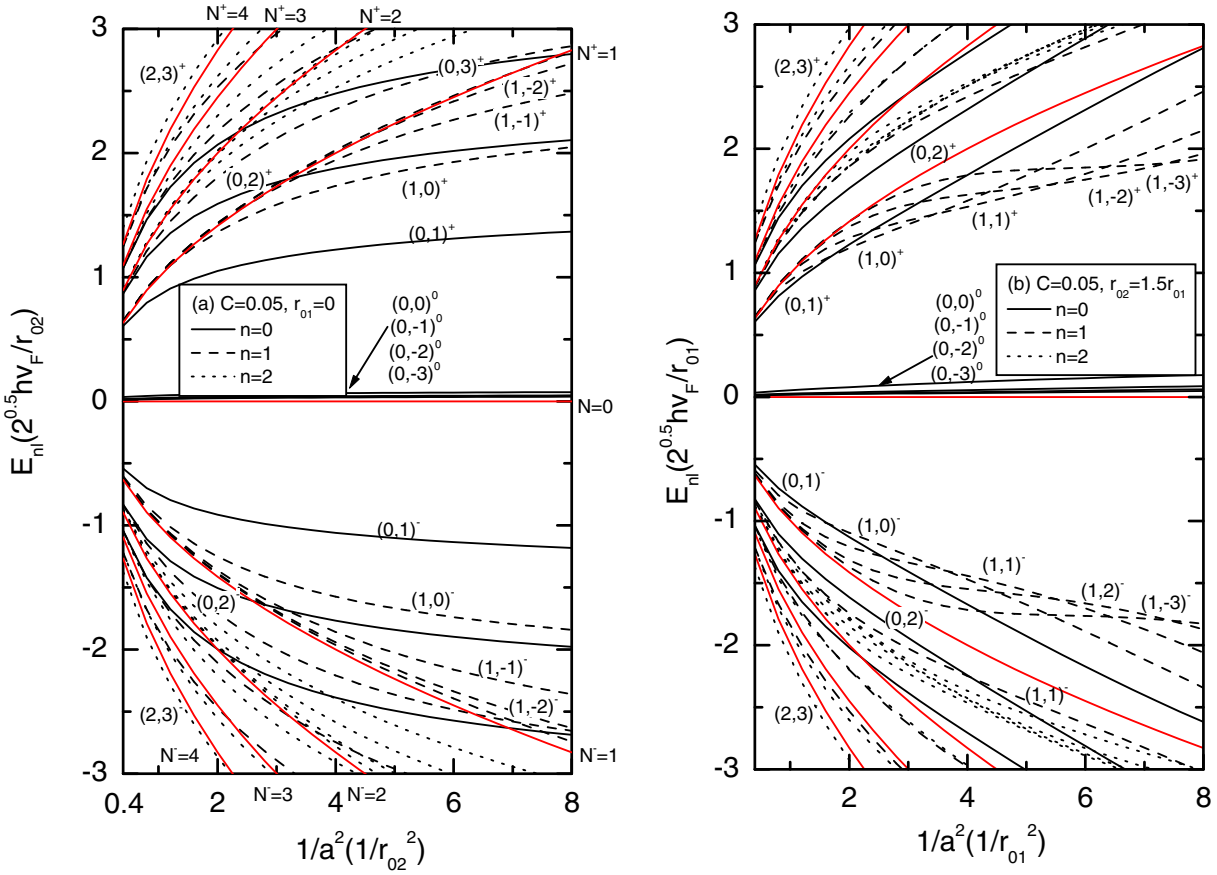

Fig. 2. (Color online) Same as those in Fig. 1 but with $C = 0.05$.

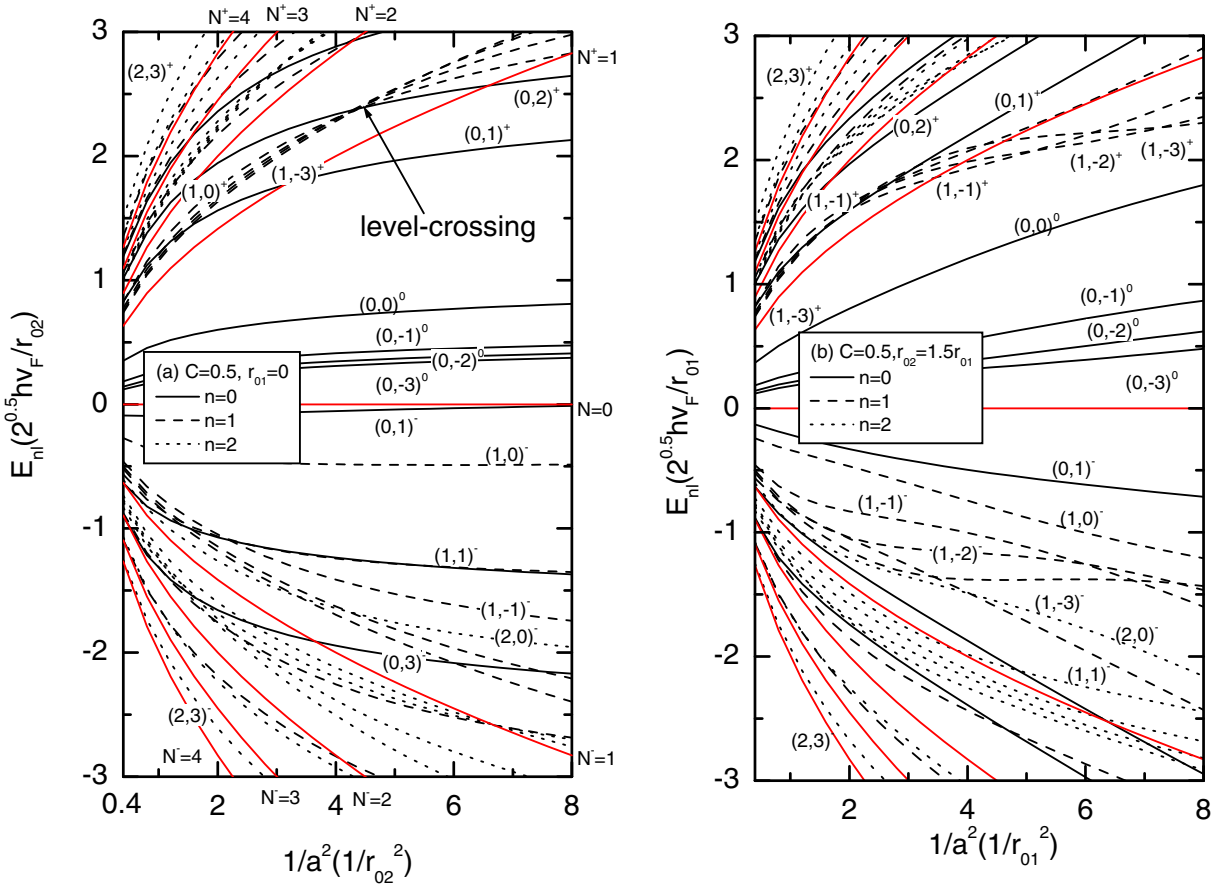

Fig. 3. (Color online) Same as those in Fig. 1 but with $C = 0.5$.

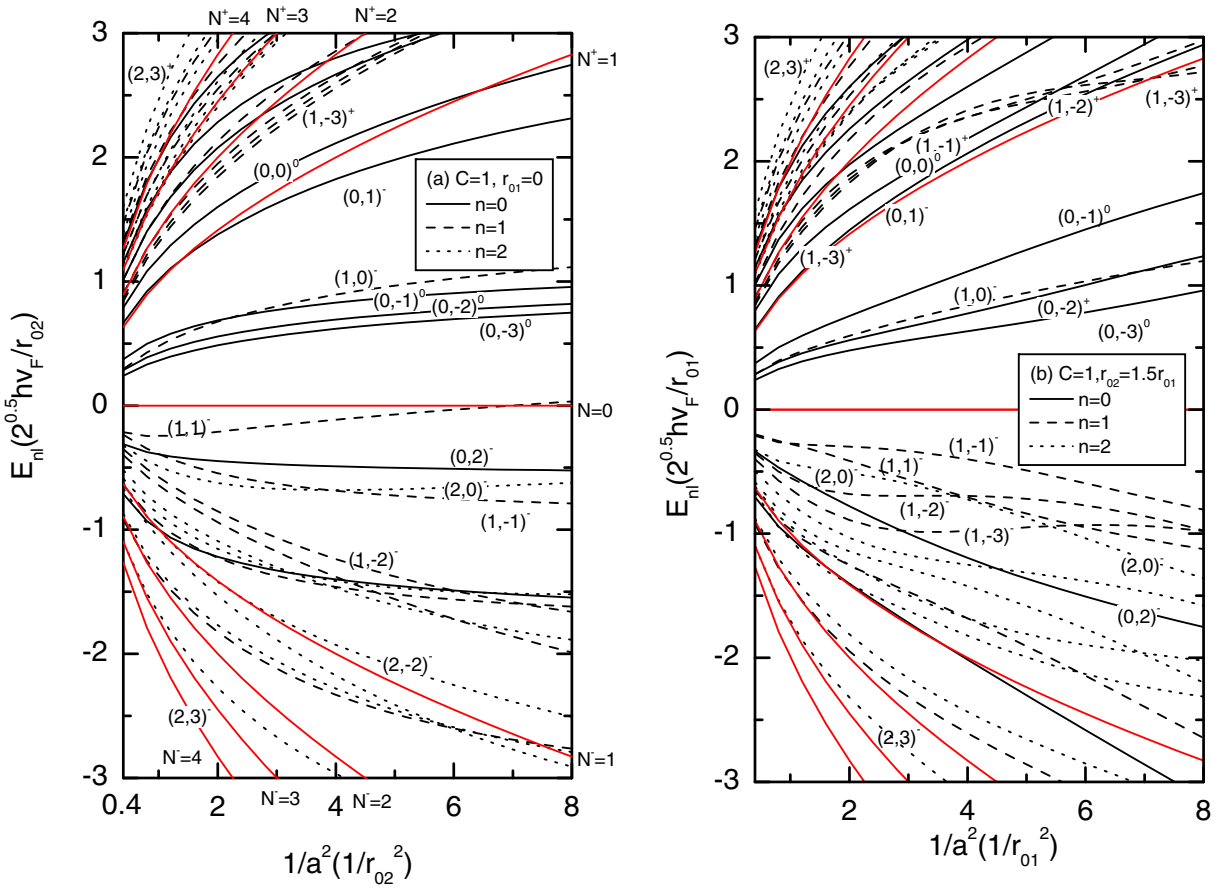

Fig. 4. (Color online) Same as those in Fig. 1 but with $C = 1$.

centrifugal barrier and the electron is much closer to the center of the impurity in this state than in the other angular momentum states. As a result, the electron becomes more unstable, and the $(0,0)^0$ state thus has the highest energy among the lowest LL, and $(0,-3)^0$ is left as the ground state. Furthermore, the stronger the magnetic-field confinement, the closer the electron is pushed toward the on-center impurity, leading to the increase of the electron-impurity repulsion which shifts these angular momentum states further upward.

Now, we focus on the first LL ($N = 1$). When the Coulomb interaction is sufficiently weak ($C = 0.05$), as in Fig. 2, the qualitative features of the first LL ($N = 1$) for both the magnetic dot and ring systems are similar to those in the impurity-free cases,[13] only having small shifts upward for both positive and negative energy states. In the case of the magnetic ring [Fig. 2(b)], for sufficiently weak fields, the angular momentum states are in general far away from the magnetic ring region, and the electron moves in a uniform field outside the ring region; therefore, the angular momentum states resemble the bulk LL and their energies are close the bulk LL energies. As the magnetic field increases, the confinement effect of the magnetic field, which resembles that of a harmonic potential, pushes the electron closer to the ring region, where the magnetic field is zero. As a consequence, the electron energy is lower than the bulk LL energy. When the magnetic field is further increased, the field confinement effect pushes the electron closer to the center of the ring, where the magnetic field is nonzero, and the electron moves in a uniform magnetic field again. The electron energy level then moves towards the bulk LL. In other words, when the magnetic field gradually increases, the eigenenergies for the angular momentum states start to deviate from the bulk LL at different magnetic fields and then move towards the bulk LL again at some larger fields. This shift in the eigenenergies leads to angular momentum state transitions, i.e.,

$$(0,1) \xrightarrow[\approx 1.632]{\approx 1.713} (1,0) \xrightarrow[\approx 3.664]{\approx 3.416} (1,-1)$$
$$\xrightarrow[\approx 5.495]{\approx 5.430} (1,-2) \xrightarrow[\approx 7.422]{\approx 7.397} (1,-3),$$

where the magnetic fields r_{01}^2/a^2 just above and below the arrows indicate the transition points between two angular momentum states for both the positive- and negative-energy states, respectively. In Fig. 2(b), since we express the magnetic field in units of the inverse of the square of the inner radius of the ring $(1/r_{01}^2)$, it can be readily deduced that the above transition points will shift toward smaller magnetic fields when r_{01} is increased and the ring region moves further away from the ring center. In the case of the magnetic dot [Fig. 2(a)], inside the dot, the magnetic field is zero and therefore the eigenenergies for all the angular momentum states simply move away from the bulk LL when the magnetic field is increased, without any angular momentum state transitions. Since the magnetic field is expressed in units of the inverse of the square of the dot radius $(1/r_{02}^2)$, it can be expected that, the larger the dot size, the weaker the magnetic field is required to push the electron deep into the zero-field dot region.

When the Coulomb interaction is increased to $C = 0.5$ for the magnetic dot with an impurity [see Fig. 3(a)], for the

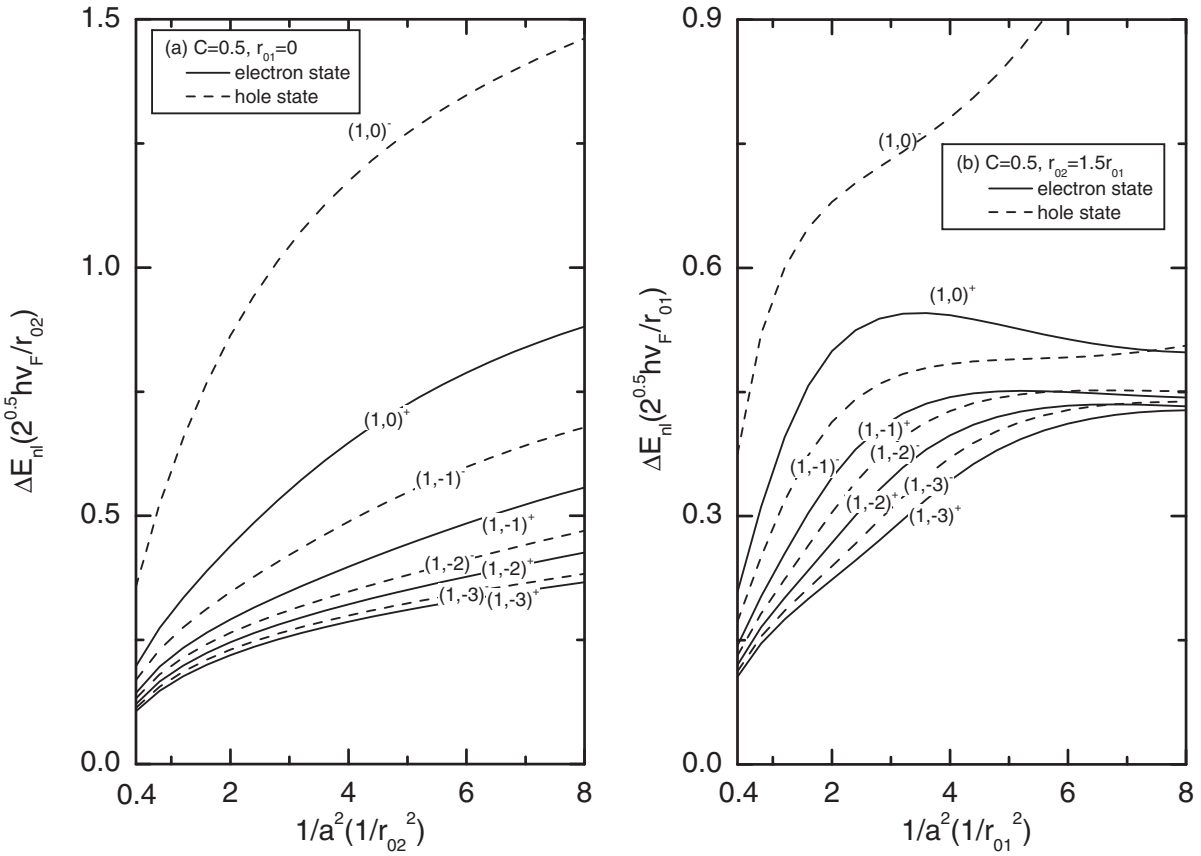

Fig. 5. Binding energies of (a) a magnetic dot and (b) a magnetic ring as functions of $1/a^2$, which is proportional to the magnetic field ($\propto B_0$).

positive energy states, there exists a sharp point of level crossing between the states $(1,0)^+$, $(1,-1)^+$, $(1,-2)^+$, and $(1,-3)^+$ at the magnetic field $r_{02}^2/a^2 \approx 4.5$. In the electron-impurity interacting systems, there are two interaction energies with opposite effects on the ordering of the angular momentum states of a given LL; one is Coulomb force of the on-center impurity and the other is the inhomogeneous magnetic field, which compete with each other. Below a critical field, i.e., $r_{02}^2/a^2 < 4.5$, the level ordering is just similar to that of the zero LL in which the Coulomb effect is dominant. When the field exceeds this critical value, the level ordering of the angular momentum states changes to that of the impurity-free dot. The level crossing effect can also be observed in the magnetic ring [Fig. 3(b)], but it is difficult to define a single critical point owing to a more complicated field profile. For the negative energy states, the level ordering or crossing features with critical points found in the positive energy states are not observed for either the dot or ring system. This is because, the hole impurity interaction energy is negative, having effects just opposite to those of the positive energy states.

When the Coulomb interaction is increased to $C = 1$ [Fig. 4(a)], the critical point will shift to $r_{02}^2/a^2 > 6$ (not shown in the figure) for the magnetic dot with an impurity, but features similar to those in cases of weak Coulomb interaction can still be observed in the magnetic ring with the impurity [Fig. 4(b)]. On the whole, the stronger the Coulomb interaction, the larger the value of the critical point is. Note that, both the states $(0,1)^-$ and $(1,0)^-$, originally degenerate in the first LL ($N^- = 1$), now increase in eigenenergies to that above the zero bulk LL ($N = 0$) when the Coulomb interaction is sufficiently strong, as can be seen in the results for $C = 1$ in Fig. 4 for both the magnetic dot and ring systems.

Finally, in order to see the effect of only the Coulomb potential on the low-lying spectra, we define the binding energy $\Delta E_{(n,l)^\pm}$ as the difference in the energy between the states with and without the Coulomb potential. This energy can be used as an indicator of the change of the electron position since the Coulomb potential is inversely proportional to r. Using the dot and ring systems with the Coulomb interaction parameter $C = 0.5$ as examples, we plot their binding energies in Figs. 5(a) and 5(b), respectively. When the magnetic field increases, the electron is pushed towards the on-center impurity. From the figures, we see that for the negative angular momentum states the binding energies in general start to increase and finally reach some constant values, particularly for the magnetic ring system in Fig. 5(b). Apart from the effect of the strong Coulomb potential, the main reason for the behavior is that, the magnetic field at the center region tends to repel the electron in the ring region with a zero magnetic field from entering it. Furthermore, two more notes for the binding energies to be made here are that (a) the negative energy states have a higher binding energy than the positive energy ones, since the negatively charged impurity attracts the hole in the negative energy states causing a stronger Coulomb potential effect, and (b) the lower angular momentum states $|l|$ have a higher binding energy since they are much closer to the center of the system and nearer to the on-center impurity according to the expression of orbit radius.

In summary, using direct diagonalization, the low-lying spectra of single electron magnetic dot and ring systems with

an on-center negatively charged Coulomb impurity have been calculated and studied. We give several concluding remarks drawn from our numerical results as follows.

1. In the presence of an impurity, the electron–hole symmetrical structure for all the spectra is broken due to the Coulomb interaction between the electron and the impurity, and the original zero energy state becomes nondegenerate and splits into discrete angular momentum states or electron-like states.
2. For the positive energy states of neighboring higher LLs, the effect of the impurity on the ordering of low-lying levels below certain magnetic fields becomes important, when the Coulomb interaction is sufficiently strong, regardless of the magnetic field profile.
3. From the above analysis, when a negatively charged impurity is replaced by a positively charged one, it can be expected that, the spectra for the positive energy states and negative energy states are simply reversed, and the zero energy states are converted into hole-like states.

Acknowledgment

This work is supported by the General Research Fund of the Research Grants Council of Hong Kong SAR, China, under Project No. CityU 100311/11P and National Natural Science Foundation of China (NSFC, Grant No.: 11274260).

*mesimon_hk@yahoo.com.hk
†apkschan@cityu.edu.hk

1) For reviews, C. W. J. Beenakker, Rev. Mod. Phys. **80**, 1337 (2008); A. H. C. Neto, F. Guinea, N. M. R. Peres, K. S. Novoselov, and A. K. Geim, Rev. Mod. Phys. **81**, 109 (2009); D. S. L. Abergel, V. Apalkov, J. Berashevich, K. Ziegler, and T. Chakraborty, Adv. Phys. **59**, 261 (2010); N. M. R. Peres, Rev. Mod. Phys. **82**, 2673 (2010); M. O. Goerbig, Rev. Mod. Phys. **83**, 1193 (2011); V. N. Kotov, B. Uchoa, V. M. Pereira, F. Guinea, and A. H. C. Neto, Rev. Mod. Phys. **84**, 1067 (2012).
2) K. S. Novoselov, A. K. Geim, S. V. Morozov, D. Jiang, Y. Zhang, S. V. Dubonos, I. V. Grigorieva, and A. A. Firsov, Science **306**, 666 (2004).
3) K. S. Novoselov, A. K. Geim, S. V. Morozov, D. Jiang, M. I. Katsnelson, I. V. Grigorieva, S. V. Dubonos, and A. A. Firsov, Nature **438**, 197 (2005).
4) O. Klein, Z. Phys. **53**, 157 (1929).
5) A. De Martino, L. Dell'Anna, and R. Egger, Phys. Rev. Lett. **98**, 066802 (2007).
6) A. De Martino, L. Dell'Anna, and R. Egger, Solid State Commun. **144**, 547 (2007).
7) L. Dell'Anna and A. De Martino, Phys. Rev. B **79**, 045420 (2009).
8) T. K. Ghosh, J. Phys.: Condens. Matter **21**, 045505 (2009).
9) D. Wang and G. Jin, Phys. Lett. A **373**, 4082 (2009).
10) Ş. Kuru, J. Negro, and L. M. Nieto, J. Phys.: Condens. Matter **21**, 455305 (2009).
11) M. R. Masir, A. Matulis, and F. M. Peeters, Phys. Rev. B **79**, 155451 (2009).
12) C. M. Lee, R. C. H. Lee, W. Y. Ruan, and M. Y. Chou, J. Phys.: Condens. Matter **22**, 355501 (2010).
13) C. M. Lee, R. C. H. Lee, W. Y. Ruan, and M. Y. Chou, Appl. Phys. Lett. **96**, 212101 (2010).
14) V. M. Pereira, J. Nilsson, and A. H. C. Neto, Phys. Rev. Lett. **99**, 166802 (2007).
15) Y. Zhang, Y. Barlas, and K. Yang, Phys. Rev. B **85**, 165423 (2012).
16) R. Yagi and Y. Iye, J. Phys. Soc. Jpn. **62**, 1279 (1993).
17) P. D. Ye, D. Weiss, R. R. Gerhardts, M. Seeger, K. von Klitzing, K. Eberl, and H. Nickel, Phys. Rev. Lett. **74**, 3013 (1995).
18) S. Izawa, S. Katsumoto, A. Endo, and Y. Iye, J. Phys. Soc. Jpn. **64**, 706 (1995).
19) N. Kim, G. Ihm, H.-S. Sim, and K. J. Chang, Phys. Rev. B **60**, 8767 (1999).
20) S. J. Lee, S. Souma, G. Ihm, and K. J. Chang, Phys. Rep. **394**, 1 (2004).